

## 12D4-3

### Transverse-mode and Polarization Characteristics of 1.55 $\mu$ m Micromachined VCSELs

K. Hasebe<sup>1</sup>, W. Janto<sup>1</sup>, N. Nishiyama<sup>2\*</sup>, C. Caneau<sup>2</sup>, T. Sakaguchi<sup>1</sup>, A. Matsutani<sup>1</sup>, F. Koyama<sup>1</sup> and C. E. Zah<sup>2</sup>

<sup>1</sup>Microsystem Research Center, Tokyo Institute of Technology  
4259-R2-22 Nagatsuta, Midori-ku, Yokohama, 226-8503, Japan  
TEL: +81-45-924-5077, FAX: +81-45-924-5977

<sup>2</sup>Corning Incorporated, SP-PR-02-3, Corning, NY 14831, USA  
\*Presently at Tokyo Institute of Technology

Email: [hasebe.k.aa@m.titech.ac.jp](mailto:hasebe.k.aa@m.titech.ac.jp)

**Abstract:** We present the transverse-mode and polarization characteristics of 1.55- $\mu$ m micromachined VCSELs. The addition of a micromachined structure designed for athermal operations results in single transverse-mode and stable-polarization operation with an orthogonal polarization suppression ratio of over 20 dB

#### 1. Introduction

Long wavelength VCSELs are attractive for use in various applications such as local area networks and optical sensors because of potentially low manufacturing cost and low power consumption. We have fabricated micromachined VCSELs with very low rate of wavelength variation with temperature [1]. To utilize single mode VCSELs in photonic networks, both single mode operation and polarization stability are desired. However, the conventional VCSELs need a small diameter of current-injection area to achieve single mode operation, for instance, a tunnel junction less than 5  $\mu$ m in diameter for 1.55  $\mu$ m InP VCSELs [2]. To control the polarization of output light, there are several ways such as non-cylindrical resonators [3], externally applied stress [4], and so on.

In this paper, we demonstrate 1.55- $\mu$ m single mode micromachined VCSELs with low threshold current and stable polarization. The integration of a micromachined structure enables high suppression of high-order transverse modes and orthogonal polarization state.

#### 2. Device structure

Figure 1 shows the schematic structure of the micromachined VCSELs. The base structure of the devices was grown in Corning Incorporated, and is similar to that of a conventional InP-based VCSEL with tunnel junction [1]. The cantilever consists of 5.5-pairs GaInAsP/InP DBR and an InP thermal stress control layer which were grown on a GaInAs sacrificial spacer layer above the active region. A 3-pairs Si/SiO<sub>2</sub> dielectric mirror was deposited on the head of the cantilever to increase the reflectivity. Figure 2 shows the SEM view of (a) DBR mirror on the head of freely suspended cantilever and (b) a fabricated micromachined VCSEL. The mirror diameter and cantilever length are 16  $\mu$ m and 95  $\mu$ m, respectively.

#### 3. Characterization

To evaluate the characteristics of the micromachined VCSELs, we compared them with conventional structure VCSELs fabricated using the same wafer. The conventional VCSELs were fabricated by etching

both cantilever and spacer layer and then depositing a 4-pairs Si/SiO<sub>2</sub> mirror. Figure 3 shows the I-L characteristics of conventional and micromachined VCSELs for 5- $\mu$ m and 7- $\mu$ m tunnel junctions. The threshold currents of micromachined VCSELs are lower than those of conventional VCSELs because of the higher reflectivity of the top mirror. The low threshold (300 $\mu$ A) for the 5  $\mu$ m device shows the low excess loss of the micromachined structure. The low output power would be improved by optimizing the top mirror reflectivity. Lasing spectra of both VCSELs at 4-mA current are shown in Fig. 4 (a) and (b). The micromachined VCSEL with 5- $\mu$ m tunnel junction exhibits an SMSR of  $\sim$ 50 dB while the conventional VCSEL shows higher-order modes. The air cavity of the micromachined structure is expected to provide an excess diffraction loss for higher-order modes.

To investigate the polarization characteristics for both VCSELs, we measured their I-L characteristics through a polarizer. We adjusted the orientation of the polarizer with respect to the crystal axis of the substrate. Figures 6(a) and (b) show polarization-dependent I-L characteristics of conventional and micromachined VCSELs with 5- $\mu$ m diameter tunnel junctions. The direction of a polarization state is along the [011] crystal direction as shown in the inset. The micromachined VCSEL exhibits a single transverse mode with an orthogonal polarization suppression ratio (OPSR) of over 20 dB while that of the conventional VCSEL is only  $\sim$ 4 dB at the same current of 4 mA. The physical understanding of the polarization stability of micromachined VCSELs is open for discussions.

#### 4. Conclusion

We demonstrated polarization controlled single mode 1.55- $\mu$ m VCSELs with a micromachined structure. The output light was polarized along a fixed direction with an orthogonal polarization suppression ratio of over 20 dB. We expect athermal VCSELs with single mode and stable-polarization operation.

#### References

- [1] W. Janto, K. Hasebe, N. Nishiyama, C. Caneau, T. Sakaguchi, A. Matsutani, F. Koyama and C.E. Zah, IEEE International Semiconductor Laser Conference, PD1-1, 2006.
- [2] N. Nishiyama, C. Caneau, G. Guryanov, X.S. Liu, M. Hu and C.E. Zah, Electron. Lett., 39, pp. 437-439, 2003.

[3] K.D. Choquette and R.E. Leibenguth, IEEE Photon. Technol. Lett., 8, pp. 40-42, 1994  
 [4] F. Monti di Sopra, M. Brunner and R. Hövel,

IEEE Photon. Technol. Lett., 14, pp. 1034-1036, 2002.

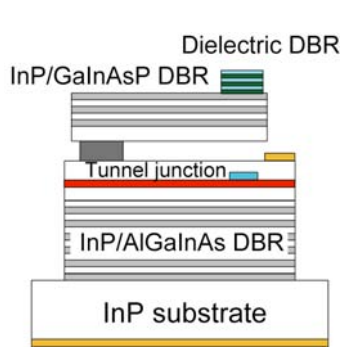


Fig. 1 A schematic structure of micromachined athermal InP VCSEL.

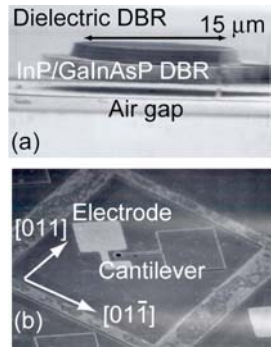


Fig. 2 SEM views of a fabricated micromachined InP VCSEL

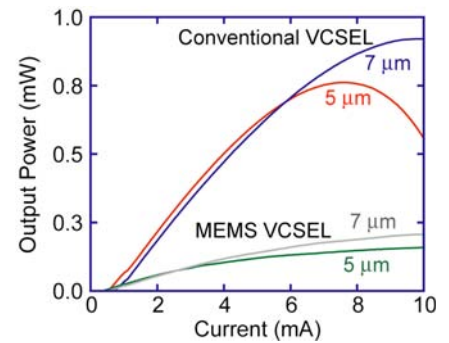


Fig. 3 I-L characteristics of conventional and micromachined VCSELs with 5- $\mu\text{m}$  and 7- $\mu\text{m}$  tunnel junctions.

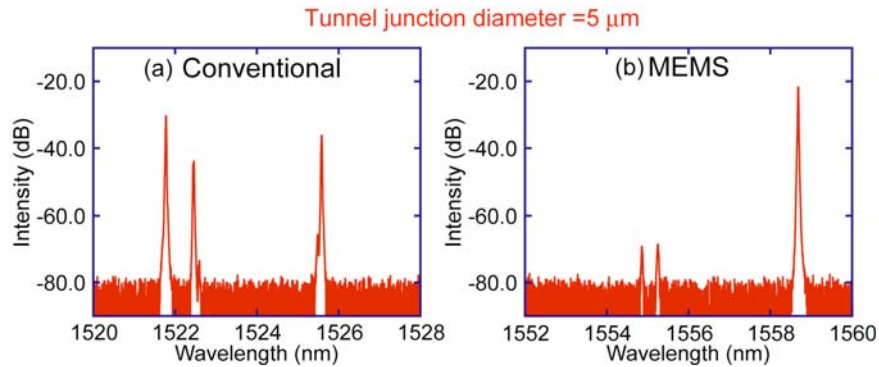


Fig. 4 Lasing spectra of conventional and MEMS VCSELs with tunnel junction of 5  $\mu\text{m}$  at 4-mA current.

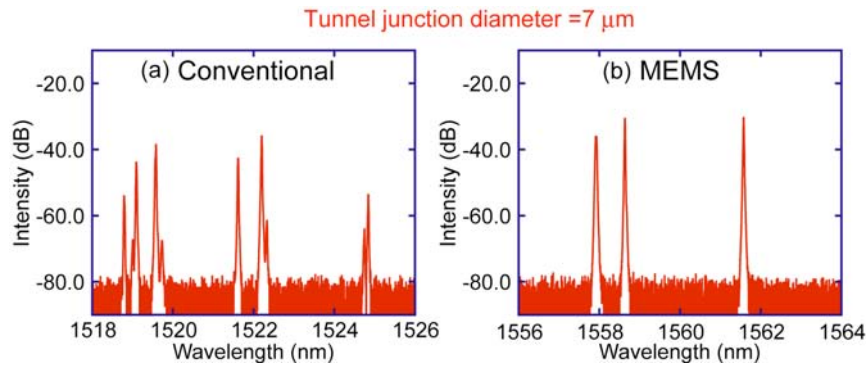


Fig. 5 Lasing spectra of conventional and MEMS VCSELs with tunnel junction of 7  $\mu\text{m}$  at 4-mA current.

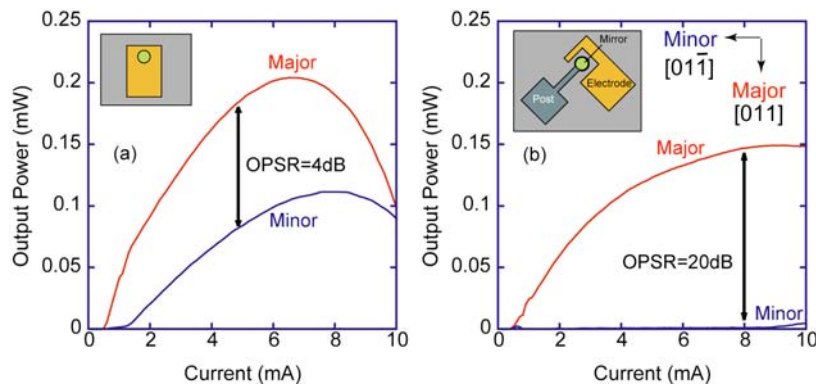


Fig. 6 Polarization characteristics of (a) conventional and (b) MEMS VCSELs.